# Classical dynamics of electrons in quantized-acoustoelectric-current devices

A. M. Robinson and C. H. W. Barnes
*Cavendish Laboratory, University of Cambridge, Madingley Road, Cambridge CB3 0HE, United Kingdom*
(Received 31 August 2000; published 4 April 2001)

We present a numerical study of the classical dynamics of interacting spinless electrons in quantized-acoustoelectric-current devices. In these devices, a surface acoustic wave (SAW) captures electrons from a two-dimensional electron gas (2DEG) and transports a fraction of them through a narrow depleted constriction. If the same number of electrons are transported in each cycle, a quantized current will result. In our model, each SAW minimum captures ~30 electrons as the SAW maximum behind it passes through the 2DEG chemical potential. It then moves toward the center of the constriction losing on average one electron every 3 ps as it becomes smaller. For temperatures below ~1.7 K the electrons form a crystal, which heats up to this temperature through the equipartition of excess potential energy produced by the loss of electrons. Thermal excitation out of the minima then results in variations in the number of electrons transported. At temperatures above ~1.7 K the electrons are in a more liquidlike state and evaporative cooling occurs. The dependence of acoustoelectric current on the constriction potential and the temperature are found to be in good agreement with experiment.

DOI: 10.1103/PhysRevB.63.165418 PACS number(s): 85.35.Gv, 73.23.Hk, 73.50.Rb, 45.50.−j

## I. INTRODUCTION

Quantized acoustoelectric current devices are currently being developed as a possible means of producing a standard of electrical current.[1–9] These devices operate at gigahertz frequencies and a single device delivering one electron per cycle can produce a current large enough to be measured with an accuracy suitable for metrological applications. Competing devices such as the electron pump,[10,11] which at present are more accurately quantized, are fundamentally restricted to megahertz frequencies so that thousands of devices would need to be operated in parallel in order to produce a similar current. The realization of a standard of current is important because it would close the ''metrological triangle'' of resistance, voltage and current measurements or could alternatively be used to obtain a measure of the charge of an electron.

Metrological applications ideally require the accuracy of current-standard devices—the precision to which the current they produce is defined—to be better than one hundred parts per billion. For a quantized-acoustoelectric-current device to operate at this level of precision, the design will need to take into account all possible error mechanisms, and hence every aspect of the dynamics of the electrons as they are transported through the constriction will need to be understood.

The properties of quantized-acoustoelectric-current devices have been extensively investigated since the first realization of such a device in 1996.[1–9] A schematic diagram of a typical device is shown in Fig. 1. It consists of a $GaAs/Al_xGa_{1-x}As$ heterostructure containing a two-dimensional electron gas (2DEG) that is formed into a mesa by wet etching and further patterned with a metallic surface split-gate. When a sufficiently large negative voltage is applied to the split gate, a narrow depleted constriction is defined that connects two regions of 2DEG.

An interdigitated transducer powered by a microwave frequency source is used to launch a surface acoustic wave (SAW) toward and parallel to the constriction, and the piezoelectric properties of GaAs and $Al_xGa_{1-x}As$ cause a wave of electrostatic potential to travel along with this SAW. The potential modulation due to the SAW, together with the potential due to the constriction, produces a series of quantum dots, each one corresponding to a particular minimum of the SAW potential, which pass through the constriction. Each quantum dot fills with electrons on the left side of the constriction (see Fig. 1), and empties on the right, thereby producing a current. Each such event is independent because the SAW wavelength is approximately the same as the length of the constriction so that the constriction only contains one quantum dot at a time.

In principle these devices could produce a standard of current because each quantum dot that passes through the constriction should be described by an essentially identical time-dependent potential function, and therefore over some range of external parameters it should be possible to ensure that each dot captures and transports the same *integer* number of electrons $n$ from the left 2DEG to the right 2DEG. This would produce a quantized current $I=nef$, where $f$ is the SAW frequency and $e$ is the electronic charge. Experimentally, the depth and size of the dots are altered by sweeping the split-gate voltage or SAW power, and a series of

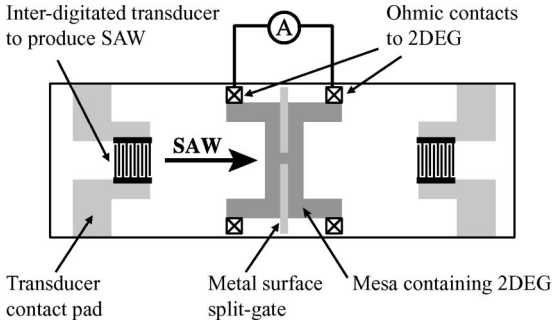


FIG. 1. Schematic diagram of a quantized-acoustoelectric-current device.

 

current plateaus corresponding to a range of values of $n$ is observed.

The best quantized-acoustoelectric-current devices to date have produced current plateaus that were flat to within 100 parts per million,[4–7] although as yet the current on the plateau has only been demonstrated to be equal to $ef$ to approximately 160 parts per million.[8] However, many devices have shown much poorer plateaus.[12] The theoretical maximum possible accuracy of these devices is not known, and indeed, even the nature of the error mechanisms is not fully understood.

When the first observation of quantized current produced by a SAW-based device was reported by Shilton *et al.*,[1] they suggested that the mode of operation of the devices is as follows: each quantum dot formed by the SAW and the constriction initially contains more than one electron; as it moves toward the center of the constriction its potential minimum passes above the 2DEG chemical potentials and its size decreases; the decrease in size causes electrons to be forced to leave the dot because of the Coulomb repulsion between them; and the Coulomb interaction fixes the final number of electrons left in each of the dots.

Recent theoretical works have added to this understanding by considering quantum mechanical tunneling as an error mechanism. An exact time-dependent one-dimensional single-particle model by Maksym[13] finds that the electrons that are transported through the constriction are those in the lowest energy states of the SAW minima. The error mechanism for the first plateau is tunneling through a ''leaky'' Landau-Zener process:[14] when a state in the dot anticrosses with a continuum state in the 2DEG, some part of the electron probability escapes. Flensberg *et al.*[15] consider a model that includes both tunneling via the WKB approximation and the Coulomb-blockade effect. In their model, they propose that the rapid decrease in tunneling coupling that occurs after the definition of the quantum dot prevents thermal equilibrium between the dot and the 2DEG. This then leads to fluctuations in the occupation number of the dot and therefore to deviations from the quantized values of the acoustoelectric current.

A third study consists of two papers by Aizin and co-workers.[16,17] Of particular significance is that they find that electrons are transported through the constriction out of equilibrium with the 2DEG's in a manner similar to that proposed in the original experimental paper.[1] In calculating the acoustoelectric current, Aizin and co-workers[16,17] use a quasistatic approximation, and tunneling out of the dot is calculated in the WKB approximation. The first paper considers just a single electron, but in the second paper two electrons are considered and the exact Coulomb interaction between them is included. All of the above works show that if tunneling could be made to be the dominant error mechanism then current quantization in these devices which satisfy the requirements of metrologists.

In this paper we develop a 2D interacting classical model for the study of quantized-acoutoelectric-current devices that allows us to look in detail at electron dynamics in the capture process. In Sec. II we discuss the form of the effective potential produced by the constriction and the moving SAW, and use experimental observations to parametrize it. The scheme used to calculate the acoustoelectric current and the role of chaos are described in Sec. III, and in Sec. IV we give a detailed account of the motion of the electrons as they pass through the constriction. In Sec. V we give results for current versus barrier height and compare our results with published experimental data. The transport on the first current plateau is investigated in Sec. VI by analyzing the variations of the potential and kinetic energies of the electrons with time, and the origin of errors in the number of electrons transported is explained. In Sec. VII we discuss error mechanisms on higher current plateaus, and Sec. VIII describes the dependence on the initial temperature of the electrons that our model predicts. Section IX gives a justification for the use of a classical model and Sec. X is a summary of our findings.

## II. THE EFFECTIVE POTENTIAL

The precise form for the effective potential in a split-gate constriction is still a matter for debate.[18] The contribution of trapped electrons on the semiconductor surface, the location and state of ionization of donor atoms, and the strain around split-gate are all unknowns for a specific device. However, for our purposes a precise form for the effective potential is not important since we are only concerned with understanding the processes that occur when electrons are forced through a constriction by a SAW and are not attempting to model specific experimental devices to high degrees of accuracy.

Typically, the metallic surface split-gate used in the devices is 0.7 $\mu$m long with a 1-$\mu$m-wide gap, and the 2DEG is situated 0.1 $\mu$m below the surface. The split-gate is operated well beyond conductance pinch-off (by typically a couple of tenths of a volt beyond the pinch-off voltage in the absence of a SAW) so that the edge of the depleted region is well away from the edge of the surface metal and therefore has a smooth shape. In this regime, the potential from the split gate may be approximately represented using a simple combination of Gaussian functions. The SAW is added as a sine wave, producing a total potential,

$$V_{tot}(x,y) = e^{-x^2/2l^2}\left[V_1 - (V_1 - V_2 - V_0)e^{-y^2/2w^2}\right] - A\cos[(2\pi x/\lambda) - 2\pi f t] - V_0, \quad (1)$$

where the $x$ and $y$ axes are in the plane of the 2DEG with the $x$ axis parallel to the direction of propagation of the SAW and the point (0,0) is at the center of the constriction. In the absence of the SAW, $V_1$ is the height of the barrier under the surface metal and well away from the constriction, $V_2$ (the ''barrier height'') is the height of the center of the constriction above the 2DEG chemical potentials $V_\mu = 0$, and $-V_0$ is the limiting value of the potential as $|x| \to \infty$. The length of the constriction is determined by $l$, $w$ determines its width, $A$ is the SAW potential amplitude, $\lambda$ is the SAW wavelength, and $f$ is the SAW frequency.

Below the 2DEG chemical potentials $V_{tot}$ will be screened by electrons, but we do not include this in $V_{tot}$ because the form of the potential in the 2DEG region is irrelevant to our calculations since we are only interested in

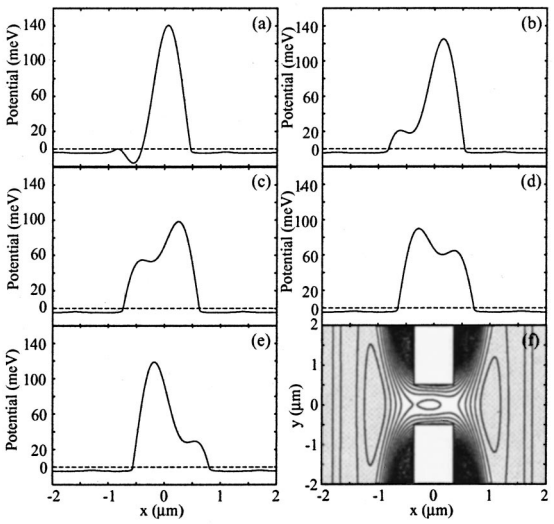


FIG. 2. Effective potential through the center of the constriction in the direction of SAW propagation for times (a) 0.595 ns, (b) 0.645 ns, (c) 0.695 ns, (d) 0.795 ns and (e) 0.845 ns (the zero of potential has been chosen to be at the 2DEG chemical potential, and in the 2DEG region the screened potential is represented schematically), (f) contour plot of the potential at time 0.73 ns and relation to surface split gates (gray shows 2DEG).

the behavior of electrons in the dots, and within each dot all of the interactions between electrons are treated explicitly. In addition to this dynamic screening, the SAW amplitude will be affected by the presence of the split-gates[16] and the 2DEG. A position-dependent SAW amplitude could be trivially incorporated into our model, but we do not believe that this is necessary for our purposes since in our model the basic features of the dynamics rely only on the number of electrons that the dot can hold decreasing to some minimum value after the dot defines.

Solving the 3D Poisson equation using a Fourier method to obtain the potential in the plane of the 2DEG, we find that for the device dimensions given above, $l=0.4$ $\mu$m and $w=1.5$ $\mu$m provide a good representation of the potential in the region of interest. Experiments[4] suggest that the optimized conditions for producing a quantized current in these devices are an unscreened SAW amplitude $A$ of a few tens of meV and a barrier potential of $V_2 \sim 100$ meV. Typical split-gate voltages of $\sim -3$ V give $V_1 \sim 3000$ meV, and the SAW wavelength and frequency are typically approximately $\lambda = 1$ $\mu$m and $f=2.7$ GHz respectively.

Figures 2(a)–(e) show the effective potential $V_{tot}$ through the center of the constriction at 0.05 ns intervals during one cycle, for a SAW amplitude $A=40$ meV, a barrier potential with $V_2=100$ meV and $V_1=3000$ meV, a value $V_0=55$ meV so that the length of the pinched-off region is approximately 1 $\mu$m with no SAW present, and values for the other parameters as given above. For regions where 2DEG exists, this figure incorporates screening by the 2DEG's schematically by using a ''screening factor'' that varies linearly with the local 2DEG density. Experiments on the effect of a SAW on the conductance of an open quasi-one-dimensional channel[12,19] suggest that the screened SAW potential in the constriction is of the order of 1 meV for the values of SAW power used to generate quantized currents. Figure 2(f) shows a contour plot of $V_{tot}$ at $t=0.73$ ns, which is close to the instant when there is a quantum dot at the center of the constriction. The 2DEGs are indicated by gray shading and the split gates by white rectangles.

## III. CALCULATION OF THE CURRENT

The sequence of potentials in Fig. 2 shows that the SAW is capable of transporting electrons through the constriction since a local minimum is present throughout the cycle. An isolated quantum dot containing a number of electrons forms to the left of the constriction in Fig. 2(a). This dot then passes through the constriction taking a fraction of those electrons with it. Since the length of the constriction is approximately the same as the SAW wavelength, only one minimum passes through the constriction at a time so that in our calculations we can treat each minimum separately. For a longer constriction it would be possible for an escaping electron to interact with, or be caught in, the next minimum and this would affect the transport.

Our calculation of the current through the constriction consists of a series of simulations in which (slightly) different configurations of electrons are started in the quantum dot at the instant of its definition [Fig. 2(a)]. Their classical dynamics is then calculated until the dot has passed the center of the constriction, at which instant the rear barrier of the dot is so large that it is not possible for any electrons to escape back to the left 2DEG. The current is calculated from the total charge transported through the constriction in a given time.

Consideration of the dynamics prior to the definition of the dot is fundamentally problematic in a classical model. In the experiment the 2DEGs form Fermi liquids but in a classical model the 2DEGs would form an electron crystal at low temperatures and a Coulomb liquid at higher temperatures.[20,21] Unlike in an electron crystal or a Coulomb liquid, electrons occupying states well beneath the chemical potential in a Fermi liquid are not free to scatter. It is therefore reasonable to expect that once the combination of a SAW minimum and the constriction potential confines some electrons beneath the chemical potential, these trapped electrons will evolve with little or no excitation until they pass through the chemical potential. At the instant of definition of the quantum dot the configuration of the electrons would then be a small random perturbation away from the instantaneous quantum-mechanical ground state. For our classical model we therefore choose the initial configuration of the electrons in the quantum dot to be a small random perturbation away from the classical instantaneous ground state. By varying the size of this random perturbation we can choose the initial temperature of the electrons in the dot.

We use simulated thermal annealing[22] to determine the ground state configuration—the number of electrons and their positions—of the quantum dot at the instant it becomes defined. An example is shown in Fig. 3 for a dot containing 27 electrons and as expected it has a crystalline form with triangular coordination.[23,24] For greater than ten electrons

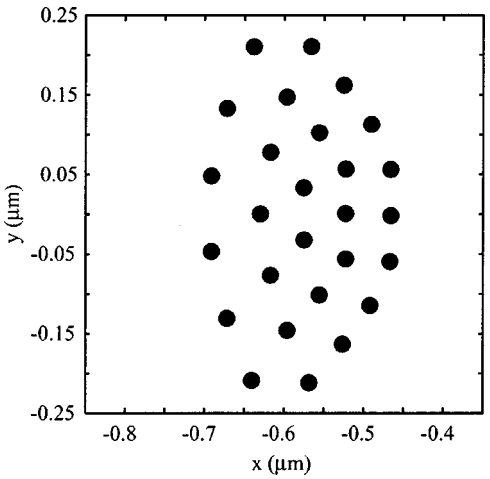


FIG. 3. Typical initial configuration of a dot containing 27 electrons.

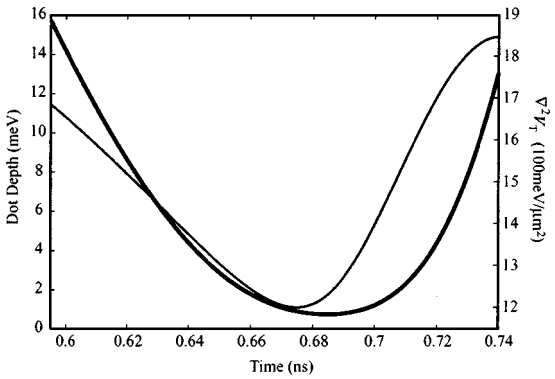


FIG. 4. Depth (left axis, thick line) and curvature (right axis, thin line) of the quantum dot versus time from when the rear barrier rises above the chemical potential to when the dot is precisely at the center of the constriction.

this method often results in different initial random seeds for the anneal producing different values for the maximum number of electrons that the dot can hold, and/or different electron configurations. This is simply because the large phase space for a large number of electrons means that the simulated thermal anneal often tends toward a local minimum of energy rather than finding the absolute minimum. This problem is alleviated by trying a large number of different initial random seeds and then choosing the final configuration that has the largest number of electrons, and the lowest potential energy for that number. The precise configuration of the many-electron initial state is not found to affect the mean number of electrons transported through the constriction when only a small fraction of the initial number of electrons are transported.

The initial velocities of the electrons are determined by evolving the dot backward in time (backward so that the dot is still large enough to hold the electrons) for a short time interval while keeping the electrons in the ground state by repeatedly minimizing their energy. The velocities are then simply calculated as the difference in positions divided by this time interval. Note that because the dot is continually changing shape, the initial velocities are of different sizes and are in different directions. The electrons, which have effective mass $m_{\rm eff}=0.067m_e$, are subjected to the force due to the potential $V_{tot}$ and the bare Coulomb forces from all of the other electrons in the dot. The relative dielectric constant of the medium is taken to be 13.0. Newton's equations of motion for the electrons are then solved using a standard library routine (NAG D02PCF) until the SAW minimum of interest has passed through the constriction, and the number of electrons transported through the constriction is then counted. For a given initial configuration, the calculation must predict that a well-defined integer number of electrons should be transported in each cycle since the equations of motion are solved exactly. However, the result is found to have an extremely sensitive dependence on the initial positions and velocities of the electrons, indicating that their dynamics is chaotic. In fact changing the initial positions by only $10^{-6}$ $\mu$m can significantly alter the positions of the electrons only 0.05 ns later, and a detailed check for convergence has been necessary. In reality the system would have a finite temperature and would be continually disturbed by phonons, electromagnetic pickup on the surface gates and connecting wires, and so on, causing the average number of electrons transported to be nonintegral. The initial ground-state positions, which typically have electron separations of 0.05–0.1 $\mu$m, are therefore calculated to a precision of only $10^{-4}$ $\mu$m using the simulated thermal anneal. These positions are then perturbed by $10^{-4}$ $\mu$m in random directions and the resulting number of electrons transported is averaged over many simulations of the motion. These perturbations away from the ground state correspond to an increase in energy equivalent to less than a few milliKelvin.

## IV. DESCRIPTION OF ELECTRON DYNAMICS

For the values of the parameters we have been discussing and a barrier height of 104 meV (chosen so that a single electron is transported), the dot initially contains 27 electrons in their classical ground state (Fig. 3). Figure 4 shows how the depth and curvature of the dot vary with time for our choice of potential. The curvature is the sum of the second spatial derivatives of the potential in the $x$ and $y$ directions at the bottom of the dot. A smaller curvature means that the potential in the dot is less steeply sloping, and for a given depth of dot the curvature therefore relates to the area of the dot. As can be seen, from the instant when the dot defines at 0.595 ns to approximately 0.68 ns the depth and curvature of the dot decrease. The decrease in depth dominates and has the effect that electrons are ejected from the dot during this interval. The rearmost electron is ejected only 2 ps after the dot defines, and leaves so quickly that the other electrons do not have time to adjust and are left in an excited configuration. The electrons move toward new equilibrium positions but because the dot continues to become more shallow, further electrons are ejected at an average rate of approximately one every 3 ps. The result of this process is that initially the motion is characterized by portions of the crystal structure ''flowing'' as the electrons try to rearrange themselves into a configuration with lower potential energy, but once the num-

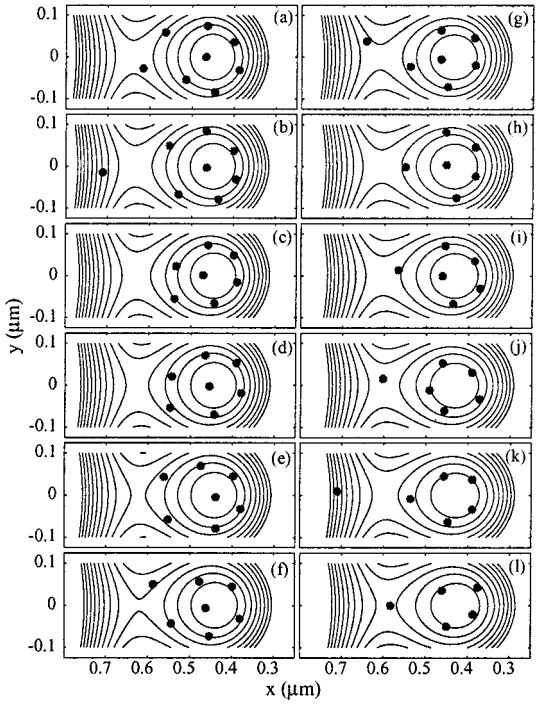


FIG. 5. Positions of the electrons (black dots) during a particular simulation for a sequence of times from (a) 0.644 ns through in 1 ps intervals to (l) 0.655 ns. The position and shape of the dot is shown by contour plots of the effective potential.

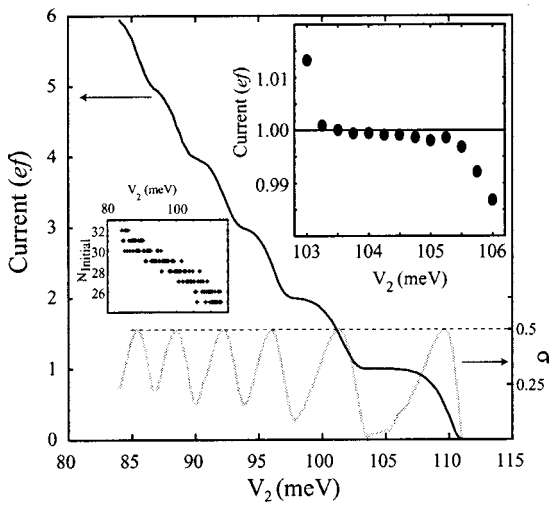


FIG. 6. Current versus barrier height determined by averaging over 10 000 simulations per point, and upper inset a close-up of the center of the first plateau. Gray line: standard deviation $\sigma$ of the number of electrons transported by individual dots, right axis. Lower inset: initial number of electrons in the dot for each value of barrier height considered.

ber of electrons drops below $\sim 10$ most or all of the electrons are seen to vibrate about local equilibrium positions. For this particular set of parameters, the dot holds only a single electron by 0.68 ns, and this electron is transported through the constriction because subsequently the dot becomes deeper and can easily accommodate it. Figures 5(a)–(l) illustrate the sequence of escape and excitation by showing the positions of the electrons during one particular simulation for a set of times from 0.644 ns when the dot is just about to lose one of eight remaining electrons through to 0.655 ns when it is losing one of five remaining electrons.

## V. CURRENT VERSUS BARRIER HEIGHT

Experimentally the current produced by a quantized-acoustoelectric-current device is measured as a function of split-gate voltage. The principal effects of changing the split-gate voltage are to change the height and gradient of the barrier, which for our choice of potential function corresponds to changing $V_2$. Dzurak *et al.*[25] found that for a pinched-off 0.3-$\mu$m wide split-gate, the height of the barrier in eV is approximately three quarters of the difference between the gate voltage (in volts) and the value of the gate voltage at conductance pinch-off. It is plausible that such a linear relationship should hold for the wider split gates used in quantized-acoustoelectric-current devices, although the constant of proportionality would be expected to be dependent on the gate geometry. The data presented in this paper has ''barrier height'' as the independent variable; for the purposes of comparing this data with experiments we assume that the linear relationship is valid and that the constant of proportionality is of the order of 1 eV/V.

Figure 6 shows a plot of current against barrier height $V_2$ for the parameters given in Sec. II obtained by averaging over 10 000 initial configurations per barrier height value. The current is the mean number of electrons transported through the constriction per cycle multiplied by $ef$. In order to show how well quantized the transport is at the level of individual dots, this figure also shows the standard deviation of the number of electrons transported per cycle. We see that on the first current plateau, the standard deviation drops to a low value, indicating that the plateau results from the majority of the dots being singly occupied rather than there being a random occupation that averages to one. For higher plateaus the minima of the standard deviation curve are at successively higher values, indicating that the performance of the device is decreasing. The standard deviation curve also shows that when the current is $(n+\frac{1}{2})ef$, each dot transports either $n$ electrons or $n+1$ electrons, so that the standard deviation of the number transported is $\frac{1}{2}$. These results could be verified experimentally by measuring the shot noise produced by these devices.

The upper inset shows just the central region of the first plateau (the ''noise'' arises from statistical errors due to the finite number of calculations), and the lower inset shows the initial number of electrons in the dot for each value of barrier height. From the smoothness of the current versus barrier height curve we see that the fluctuations in the initial number of electrons due to the performance of the simulated thermal annealing method used does not noticeably affect the current calculated.

The computation time required for these calculations has restricted the number of barrier height values ($\Delta V_2 = 0.25$ meV) and the number of simulations per barrier height (10 000) that we have considered. For a particular

value of barrier height, the accuracy to which we can specify the current and the standard deviation of the number of electrons transported per cycle, $\sigma$, is therefore limited. The precision to which we can specify the values of barrier height where the slope of the plateaus is minimized, or where $\sigma$ is minimized, is also limited. However, the data in the inset to the figure shows that the first plateau does not occur at $I=ef$ to within the accuracy of our calculations, so that increasing the numerical accuracy is not necessary. The flattest part of the first plateau is seen to be between approximately 103.5 meV and 105.25 meV, the slope of the plateau in this region being approximately 0.1%/meV. The current at the center of this region is approximately 0.1% below $ef$. The minimal value for the standard deviation of the number of electrons transported per cycle, $\sigma=0.009\,999\,5$, was found at a barrier height of 103.5 meV—at the edge of the flattest region. The current here was calculated to be $0.9999ef$, but this value and the value for $\sigma$ are subject to statistical errors arising from only one out of the ten thousand dots considered failing to transport an electron. Note that experimentally, unless an accurate measurement of the shot noise can be made, the point where the plateau is flattest rather than where $\sigma$ is minimized will have to be chosen as the point where a SAW-based current standard device is operated.

The dependence of acoustoelectric current on barrier height in Fig. 6 has a number of features that are in agreement with experiment.[1–5,8,9] The plateaus have a characteristic asymmetric shape and finite slope. Their flattest points are below the ideal ''quantized'' values, with higher plateaus becoming successively more steeply sloping and further below the ideal values. Experimentally, the points where the current takes the values $I=0.5ef$ and $I=1.5ef$ are typically separated by 20 mV in gate voltage, and the first plateau occurs roughly 200 mV beyond conductance pinchoff. In Figure 6, the separation between the $I=0.5ef$ and $I=1.5ef$ points (approximately 10 meV) compared with the distance of the first plateau beyond pinchoff (approximately 100 meV) is in agreement with these experimental values. The decreasing separation between the corresponding points for the higher plateau also agrees with experimental data. These quantities do not reflect the flatness of the plateau, but rather the form of the potential in the constriction and its variation with gate voltage, and this agreement therefore provides a partial justification for our choice of potential function. For our data, the flattest 1 meV of the first plateau has a slope of approximately 0.1%/meV; experimentally, the flattest 1 mV observed so far had a slope of approximately 0.04%/mV (Ref. 4) but other published data has slopes for the flattest 1 mV of approximately 0.09%/meV,[8] 0.2%/meV,[2] and 0.4%/meV.[5] We note that the plateaus in these papers were optimized to produce a $\sim 100\ \mu$V long region over which the current varied by $\sim 100$ ppm.

## VI. THE FIRST CURRENT PLATEAU

In order to understand what causes deviations from perfect quantization on the first plateau and to understand further details of the transport, this section looks in detail at how the potential and kinetic energies of electrons in the dot vary with time. We use the parameters given in Sec. II and a barrier of height of 104 meV so that the mean number of electrons transported per cycle is close to one.

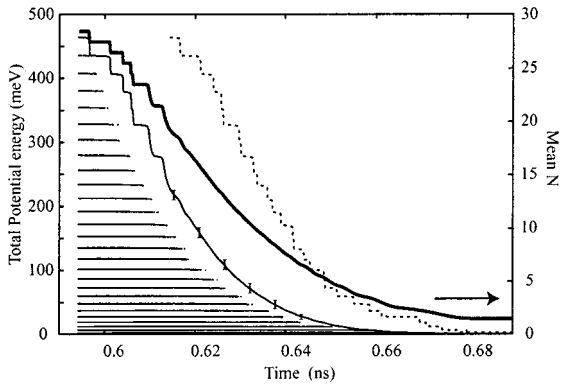


FIG. 7. Approximately horizontal solid lines: ground-state energies versus time—the lowest curve is for one electron, the next highest for two electrons, etc. Solid line: mean total potential energy versus time from time-dependent calculations, averaged over 10 000 calculations, standard deviation indicated by line thickness and vertical bars. Dashed line: curve from a single simulation, offset by 0.02 ns for clarity. Thick solid line: mean number of electrons in the dot, right axis.

### A. Potential energy

Figure 7 shows the potential energy of different numbers of electrons in the dot at a series of times for electrons that are in classical ground-state configurations. These energies are determined by simulated thermal annealing and are the sum of the potential energies due to $V_{tot}$ plus the total Coulomb potential energy of the electrons. For each time, the zero of potential is chosen so that a single electron in the dot will have zero potential energy. Unlike conventional Coulomb blockade devices[26] there is no compensating positive background charge because the dot-potential minimum is far above the 2DEG chemical potentials and therefore the increase in potential energy when an electron is added is larger if there are more electrons in the dot. The curve for a particular number of electrons terminates when the dot is too small to hold that number.

Figure 7 also shows the total potential energy of electrons in the dot when in motion, as a function of time obtained by averaging over 10 000 simulations, vertical bars indicate the standard deviation of this quantity; an example curve from a single simulation; and a plot of the mean number of electrons in the dot versus time.

The potential-energy curve obtained from a single simulation of the motion shows that the number of electrons within the dot is the dominant factor in determining the total potential energy. This is because there are distinct steps in the total potential energy corresponding to electrons leaving the dot, and these steps are aligned with the ground-state energy values. We know that the steps correspond to electrons leaving the dot from inspecting the steps in the number of electrons in the dot, as illustrated by the curves for the mean number of electrons and the mean total potential energy.

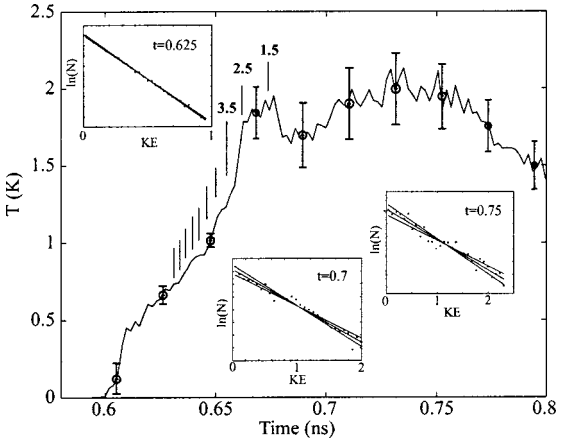


FIG. 8. Boltzmann temperature versus time, with error bars at a selection of times. Vertical lines indicate the times when electrons are most likely to leave the dot; the numbers indicate the mean occupation at these times. Insets: the distribution of kinetic energies (in units of $k_B \times 1$ K) at three chosen times, averaged over 10 000 simulations and with the number of electrons plotted on log scales. Each of the insets shows the straight lines used to obtain the Boltzmann temperature and its error.

From the data obtained by averaging over many simulations we see that for the bulk of the motion there are more electrons in the dot than the dot can actually contain in equilibrium. This is because the electrons that leave are not precisely at the edge of the dot, and hence they take a finite time to leave. Note that we are taking the edge of the dot to be at the local maximum of $V_{tot}$, which neglects the effect of the Coulomb potential from the electrons. The smoothness of the curve for the mean number of electrons within the dot shows that the chaotic nature of the motion causes the times when electrons leave to vary significantly between different calculations.

### B. Kinetic energy

Figure 8 shows the Boltzmann temperature of the electrons in the dot versus time. For each time, it was calculated from the kinetic energies of electrons within the dot in a frame moving with the instantaneous velocity of the minimum of the dot. Histograms of these kinetic energies were produced from 10 000 simulations and were fitted to the Boltzmann distribution. The insets show log plots of these histograms at three times, and each plot forms a good straight line showing that the distribution of kinetic energies of electrons in the dot is close to the Boltzmann distribution. Note that a temperature of 1 K corresponds to a speed of approximately 21 000 m/s (approximately seven times the SAW velocity) or an energy of approximately 0.09 meV.

From this figure we see that at the start of the simulations, the electrons have close to zero temperature. As the dot moves toward the center of the constriction and electrons leave the dot, the temperature of the electrons still in the dot tends to rise. At 0.685 ns the well contains exactly one electron for all the simulations and the temperature is approximately 1.7 K. Some further heating occurs up to 0.74 ns at which instant the dot is precisely in the center of the constriction, and after 0.74 ns some cooling occurs. The increase in temperature observed up to approximately 0.68 ns arises because when an electron leaves the dot it leaves so quickly that a hole is left behind in the electron crystal. Such a configuration has a higher potential energy than the instantaneous ground state energy for the number of electrons left in the dot. This results in heating because the interactions between electrons rapidly causes half of this excess potential energy to become kinetic energy: heating through equipartition of excess potential energy. When there is only one electron left in the dot, a further increase in temperature occurs due to adiabatic compression. This can be understood from Fig. 4, which shows that the curvature of the dot increases from approximately 0.68 ns to 0.74 ns. Note that this mechanism does not explain the rise in temperature during the first part of the motion because the curvature actually decreases up to a time of approximately 0.68 ns. The decrease in the apparent area of the dot that occurs while electrons leave is simply a result of the decrease in the depth of the dot; it does not reflect the shape of the potential within the dot and does not lead to adiabatic compression. After the dot has passed the center of the constriction a reduction in temperature occurs due to adiabatic expansion.

For some calculations, the chaotic nature of the motion enables the last electron left in the dot to gain enough kinetic energy to be ejected from the dot despite the fact that the height of the rear barrier is $\approx 0.75$ meV (see Fig. 4). Even though the Boltzmann temperature of the last electrons left in the dots is 1.7 K, corresponding to an energy of only approximately 0.15 meV, the Boltzmann distribution ensures that some of these electrons escape. It is this mechanism that causes the first current plateau to have a finite slope and be mostly below the correct value.

## VII. HIGHER PLATEAUS

As the height of the barrier formed by the split-gates is reduced, the dots formed by the SAW and the constriction can transport more and more electrons through the constriction. For our choice of potential this is because the slope of the potential due to the constriction decreases, leading to an increase in the minimum depth of the dot during the transport and a related increase in the area of the dot. Larger currents are desirable for metrological applications, but for the devices tested to date the accuracies of the higher plateaus have always been considerably poorer than that of the first plateau. It is important to understand the reason for this since it may then be possible to design devices where this effect is reduced or absent.

At a value of barrier height for which in ideal operation each dot should transport $n$ electrons, our model suggests that errors arise for the following reasons: a dot may transport $n+1$ electrons if the paths of the electrons are such that the extra electron does not pass close to the rear of the dot before the dot deepens again; and the dot may transport only $n-1$ electrons if one of the electrons close to the back of the dot gains enough kinetic energy to leave, or if the electrons adopt a configuration where one of the electrons can be ''pushed out'' by the others. It is ''easier'' for a dot to lose

an electron than to transport an extra electron, and this results in the current plateaus having an asymmetric shape.

The magnitude of the errors produced by the above mechanisms will depend on the following: the kinetic energy gained by the electrons as the dot moves toward the center of the constriction; the minimum height of the rear barrier of the dot that the rearmost electron sees (which is not the same as the minimum depth of the dot since it must include the potential contribution from the other electrons in the dot); the shape of the dot; and the time scale on which changes in the depth or shape of the dot occur. For our choice of potential, these quantities are roughly constant for the different plateaus and probably do not explain the worsening of higher plateaus. Indeed the effective temperature of the electrons is found to be slightly lower for higher plateaus. Instead the poorer quality of higher plateaus appears to be directly caused by the increase in the number of electrons being transported. For higher plateaus an electron is more likely to leave the dot when ideally it would be transported through the constriction for the following reasons: with more electrons there is a greater probability of one of them having sufficient kinetic energy to leave; the kinetic energy is constantly being transferred among the electrons by collisions, so that with more electrons there is a greater probability of the rearmost electron being given enough kinetic energy to leave at some time; and with more electrons there are more possible configurations that do not closely resemble the ground-state configuration so that the electrons are more likely to arrange themselves in a configuration where the rearmost electron is ''pushed out.''

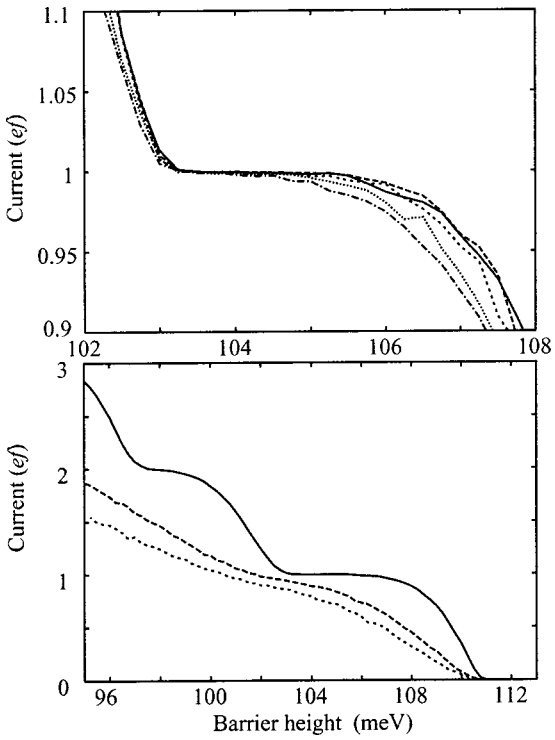


FIG. 9. Current vs barrier height for different initial temperatures, obtained by averaging over 5 000 calculations per barrier height point, top: unbroken line 0 K, long-dashed line 1 K, dashed line 2 K, dotted line 3 K, dash-dot line 4 K, and bottom: solid line 0 K, long-dashed line 50 K, dashed line 100 K.

## VIII. DEPENDENCE ON EXTERNAL TEMPERATURE

Finite initial temperature $T$ can be incorporated into our model by starting the electrons with a Boltzmann distribution of kinetic energies at temperature $2T$. The factor of 2 arises because for simplicity we can still start the electrons off with positions close to the ground-state configuration since after just the first 0.01 ns the electrons have undergone a few collisions and the motion is thermalized, with energy equally partitioned on average between kinetic and potential terms. Figure 9 shows current versus barrier height for the parameters given in Sec. II for different temperatures.

In agreement with experiment, we conclude that the plateaus do not improve significantly below $\sim 1$ K because the curves for 0 K and 1 K lie on top of each other to within their errors. This is easily explained using the results of Sec. VI: even if the electrons start off with zero temperature, their final temperature is greater than 1 K. Some caution is advised because it is not clear how the measured experimental temperature corresponds to the initial temperature of the electrons in the dot. This initial temperature will depend on the temperature of the 2DEG and on the details of how the electrons in the dot respond to the reduction in screening as the dot becomes defined. In addition, since significant heating by the applied microwave power or by attenuation of the SAW may be present, it is not known how the measured temperature corresponds to the lattice temperature or the 2DEG temperature. These temperatures will depend on the amount of heating present, the thermal contact between the sample and its holder, the rate at which heat from the 2DEG is carried away by its connecting wires, and on the rates at which the electrons can emit or absorb phonons.

Figure 10(a) shows the Boltzmann temperature versus time for dots with electrons given initial Boltzmann distributions of kinetic energies characteristic of a series of temperatures between 0 and 200 K. The parameters given in Sec. II were used, and a barrier height of 104 meV so that the current was close to $ef$ for the lower temperatures. In these curves, it can be seen that above a temperature of $\approx 1.7$ K the electrons are cooled in the initial part of the motion. This cooling is due to the fact that above this temperature the classical electron crystal melts and there is an increased probability of an electron with high kinetic energy leaving the dot. The transition from crystal to liquid does not occur suddenly at $\approx 1.7$ K in our calculations: the transition temperature is greater when a smaller number of electrons are present; and we observe that portions of the crystal may flow or break up at lower temperatures and that portions can retain crystalline characteristics at higher temperatures. At low temperatures electrons are trapped in the electron crystal and do not have sufficient kinetic energy to move over the whole of the dot. It is then just the rearmost electrons that leave first, not the most energetic and no net cooling results. Figure 10(b) shows $\Gamma$, the ratio of the potential energy of the electrons to their kinetic energy for the same set of temperatures used in Fig. 10(a). In classical 2D systems, for values of $\Gamma > 127$ the electrons form an electron crystal and for $\Gamma$

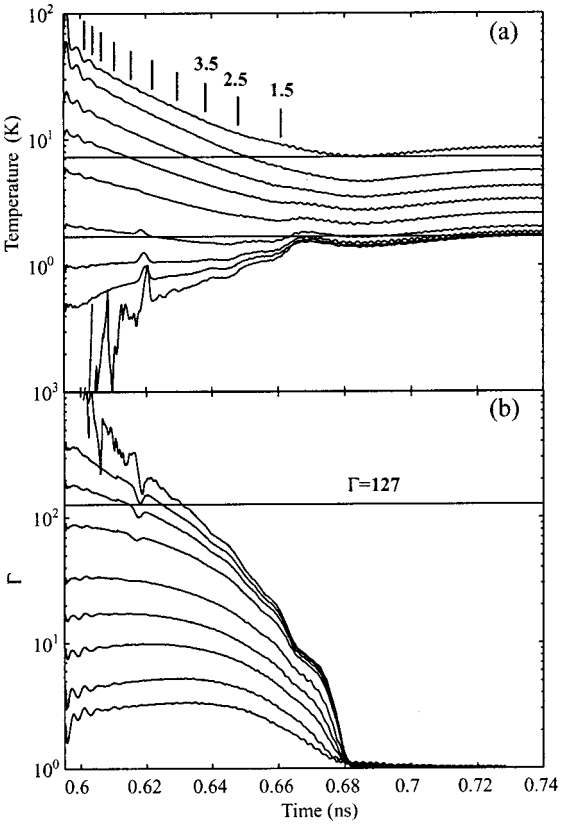


FIG. 10. (a) Boltzmann temperature vs time for a dot with electrons given an initial Boltzmann temperature of 200 K (uppermost curve), 100 K, 40 K, 20 K, 10 K, 4 K, 2 K, 1 K, and 0 K (lowest curve), obtained by averaging over 10 000 calculations. Horizontal lines indicate temperatures of 1.7 K and 7.25 K. (b) $\Gamma$, the ratio of the potential energy to the kinetic energy of electrons in the dot for the same temperatures (the uppermost curve is 0 K). The horizontal line indicates $\Gamma = 127$.

$<127$ they form an interacting electron liquid.[27] Our simulations show that this is approximately the case for our system provided the number of electrons in the dot is large.

In our model, we have not included any mechanism for electrons in the dot to absorb phonons and this has the effect that the current plateaus persist until $\sim 100$ K as can be seen in Fig. 9. At this temperature, however, the evaporative cooling we have described above cools the dot to $\approx 7$ K, which is consistent with the temperature at which experimentally the plateaus are lost. Shilton *et al.* observe a trace similar to the lowest trace in Fig. 9(b) at approximately 7 K.[1] This suggests that at 7 K the coupling to phonons is very strong and the electrons in the dot are able to equilibrate with the lattice, but the good agreement at low temperatures between our results and the experiments suggests that below $\sim 2$ K they do not have time to equilibrate. This is consistent with recent measurements of electron-phonon coupling in GaAs systems using thermopower measurements[28] and with the theory of acoustic phonon production in GaAs.[29] They quote the heat production by phonons as $dQ/dt = 270 T^5 n_e^{-3/2}$ in eV/s for $T$ in K and $n_e$ in units of $10^{15}$ m$^{-2}$. We take the time over which the dot in our calculations sheds its electrons to be 0.1 ns and take the electron density to be $0.2 \times 10^{15}$ m$^{-2}$ (this can be deduced approximately from Fig. 3). At 1 K, the formula above then gives that the energy picked up by each electron will be $3 \times 10^{-4}$ meV, an amount that could not significantly change our calculations. However, at 7 K each electron would pick up 5 meV, which would be a very significant amount of energy and suggests that at this temperature the electrons in the dot would be well equilibrated with the lattice.

## IX. CLASSICAL VERSUS QUANTUM MECHANICAL

This section looks at the connection between the expected true quantum mechanical behavior of our system and the classical dynamics that we present. The aim is to provide a justification for, and an understanding of, the quantitative agreement between experimental data and our classical simulations. We discuss the initial conditions, dynamics, and escape processes for the quantum mechanical and classical cases and consider the role of decoherence. This enables us to suggest that the heating effect discussed in Sec. VI B, the principal error mechanism at low temperatures, is relevant to experimental quantized-acoustoelectric-current devices.

### A. Initial conditions

In our calculations we start with the quantum dot formed by the SAW and the constriction containing the maximum number of electrons for its size and shape. These electrons are arranged in a configuration that minimizes the total potential energy, and are given velocities so that as the dot moves they initially remain close to a configuration of minimum potential energy.

Time-dependent noninteracting quantum-mechanical calculations[13] have shown that it is the lowest-energy electrons that are transported through the constriction. In these calculations, these electrons start in the lowest-lying bound states of the SAW minima at the entrance to the constriction. Experiments on the effect of a SAW on the conductance of an open quasi-one-dimensional channel[12,19] suggest that the screened SAW potential in the constriction is of the order of 1 meV for the values of SAW power used to generate quantized currents, so that many electrons could be trapped in such bound states. Electrons in these states are then brought up through the Fermi energy by the moving SAW potential. If Coulomb interactions were introduced into these calculations, the electrons trapped in the quantum dot should remain in the ground state because below the Fermi level there will be no free states for them to scatter into. The capture of the lowest-energy electrons is consistent with a physical picture since the SAW would not expel these electrons in favor of capturing electrons with much greater velocities (the Fermi velocity is typically 50 times the SAW velocity).

Classically, the ground-state configuration for a quantum dot formed by the SAW and constriction potentials is a Wigner cluster,[23,24] whereas quantum mechanically the ground state is an interacting liquid for the densities we are considering.[30–35] However, the quantum-mechanical ground state has the following connections to the classical ground state: the two-particle correlation function is nearly identical to the classical two particle correlation function;[32,33,35] owing

to the asymmetry of the SAW quantum dot the points where particles are most likely to be found will correlate well with the points where classical electrons are found;[33,35] and the number of electrons that the dot can hold will be very similar to the classical result since this is governed by the Coulomb energy.[32–35]

### B. Dynamics

The dynamics of an interacting many-particle system such as the one we are considering have never been calculated quantum mechanically to our knowledge, but it is likely that the time evolution of the two-particle correlation function would be very similar to that of the classical two-particle correlation function. We would expect there to be analogies of classical effects in a quantum-mechanical treatment, and indeed there must be two important similarities between the two cases. The first is that at any time during the transport, the Coulomb energy and the depth and size of the dot must be the dominant factors determining the number of electrons in the dot. Second, the processes by which electrons leave the dot occur too quickly for the remaining electrons to stay in the ground state. The velocity derived from the uncertainty principle for a confinement of 0.07 $\mu$m (the typical separation of the electrons in our simulations) is approximately 25 000 m/s, and our calculations show that electrons leave the dot on a time scale of only a picosecond. A distance of only 0.025 $\mu$m can be traveled in this time at this speed, and hence we do not expect that the wave function would be able to respond adiabatically to these changes.

### C. Tunneling

Tunneling ultimately leads to an increased depopulation of each SAW quantum dot over the classical result. This is because classically there is a sharp cutoff between states that have sufficient energy to escape the dot and those that do not. Quantum mechanically, electrons with lower energies than the classical cutoff energy may escape and electrons above the classical cutoff may be reflected back. For a parabolic barrier, if there was an even distribution of electron energies about the classical cutoff point then there would be no difference on average between the number of electrons that escape classically and the number that escape quantum mechanically. However, our calculations predict that the energy distribution closely follows the Boltzmann distribution, with a characteristic energy $k_BT<0.2$ meV, which is much less than the depth of the dot (Fig. 4). This means that in a quantum-mechanical treatment there would be more electrons attempting to leave the dot below the classical cutoff point than above it, resulting in more electrons leaving the dots on average than would classically. Nevertheless, the probability of an electron at the bottom of the dot tunneling out must be rather small because of the experimentally observed accuracies of these devices, and since the tunneling probability depends exponentially on the energy of a particle[36] then excitations of the form predicted by our model must be very important.

This suggests that tunneling should not change the general form of our results, but an example of where this does not hold is the regime where the SAW amplitude is very small. In this regime each minimum of the SAW potential is only capable of capturing one electron from the 2DEG, but if the gradient of the constriction potential is sufficiently shallow then classically each of these electrons is successfully transported through the constriction. If tunneling were included then the electrons would always escape from the dots through the small rear barriers of the dots.

### D. Decoherence

In general, the effect of decoherence on a quantum-mechanical system is to cause it to behave more classically,[37] and therefore the dynamics of the quantum dot we have been considering can be determined classically provided the dot is subject to sufficient decoherence. This could be a further justification for expecting our results to be consistent with experiment. Experimentally, the principal sources of decoherence in our system are expected to be from the process of losing electrons, coupling to acoustic phonons, and from unscreened microwave radiation. Using the results of Sec. VIII, for temperatures below 2 K each electron should pick up less than 4 $\mu$eV of energy from phonons during the 0.1 ns from when the dot defines to when it arrives at the center of the constriction. This therefore should be a negligible decohering factor. The density of microwave photons in the cavity containing the device should be small since the dimensions of the cavity are much less than the wavelength of the radiation, and they should therefore give rise to negligible decoherence.

We believe, however, that intrinsic decoherence resulting from electrons exiting the dot cannot be neglected. When electrons leave the dot by tunneling or excitation over the barrier, they will initially remain entangled with the electrons in the dot[38] but on contact with conduction electrons in the adjacent 2DEG they will decohere. This will have the effect that the electrons remaining in the dot will also partially decohere. From Fig. 7 it can be seen that on average electrons leave the dot every 3 ps and the proximity of the left 2DEG will cause decohering events to occur on this same time scale. If at some point in the motion, each electron were confined to an area given by the mean interparticle spacing ($\approx$70 nm) then the standard uncertainty relation would predict that in 3 ps they could not expand to fill the dot. This does not prove that the motion is classical but it suggests that if decoherence arising from losing electrons were to make it classical then losing electrons at such a rate would cause it to remain classical.

### E. Temperature effects

Within our model, the principal error mechanism causing deviations from quantized current plateaus is a temperature effect: at low temperatures the trapped electrons form a crystal that warms up as it passes through the constriction. The temperature at the instant when the dot has minimum depth then crucially determines the error through Boltzmann statistics. The value of $r_s\sim 7$ for the electrons in our dot is an order of magnitude smaller than that necessary for Wigner crystallization to occur, but as we have said above, (i) the

quantum-mechanical and classical two-particle correlation functions are likely to be similar, (ii) decoherence from electron loss will make this more true, and (iii) in a quantum-mechanical treatment, electrons would still be lost very rapidly thereby leaving the system with excess potential energy. The increase in temperature arises from the equipartition of this excess potential energy. A many-particle system that suddenly loses a single particle will find some way to relax, and in the absence of the possibility for it to give up acoustic phonons to the lattice or radio-frequency photons to the cavity it will probably relax by putting energy into plasma waves in the electron system. Classical and quantum-mechanical plasma frequencies are comparable and therefore this process would be expected to occur on the same time scale as our simulations. This is the heating effect we have been describing and is likely to lead to full equipartition.

## X. SUMMARY

We have presented a study of the classical dynamics of interacting electrons in quantized-acoustoelectric-current devices. In these devices, electrons caught in a SAW potential minimum are forced through a short, narrow, depleted constriction. We find that at any instant of time the combination of the SAW and the constriction produces a single moving quantum dot, the minimum of the dot corresponding to a minimum of the SAW potential. At the instant when a dot is first defined, it is relatively large and contains many electrons (for our choice of potential the number is $\sim 30$), but as it passes through the constriction it becomes smaller and electrons are forced out at an average rate of approximately one every 3 ps leading to a complicated and chaotic pattern of motion for the remaining electrons.

At low temperature, when an electron leaves the dot it leaves so quickly that a hole is left behind in the electron crystal, resulting in a configuration that has a higher potential energy than the instantaneous ground state. This results in heating because the interactions between electrons rapidly cause half of this excess potential energy to become kinetic energy. We find that even if the electrons initially have close to zero temperature, this mechanism causes them to become excited to a temperature of approximately 1.7 K. This produces errors in the number of electrons transported through excitation out of the dot. This error mechanism accounts for the experimentally observed flatness of the current plateaus, the significant worsening of higher plateaus, and the saturation of the performance of the devices at a temperature of approximately 1 K.

## ACKNOWLEDGMENTS

We thank Valery Talyanskii, Andy Schofield, Chris Ford, David Khmel'nitski and Greg McMullan for useful discussions and acknowledge the help of the Hitachi HPCF. A.M.R. thanks the National Physical Laboratory for financial support and C.H.W.B. thanks the EPSRC for finanical support. This work was funded by the EPSRC.

[1] J. M. Shilton, V. I. Talyanskii, M. Pepper, D. A. Ritchie, J. E. F. Frost, C. J. B. Ford, C. G. Smith, and G. A. C. Jones, J. Phys.: Condens. Matter **8**, L531 (1996).
[2] V. I. Talyanskii, J. M. Shilton, M. Pepper, C. G. Smith, C. J. B. Ford, E. H. Linfield, D. A. Ritchie, and G. A. C. Jones, Phys. Rev. B **56**, 15 180 (1997).
[3] V. I. Talyanskii, J. M. Shilton, J. Cunningham, M. Pepper, C. J. B. Ford, C. G. Smith, E. H. Linfield, D. A. Ritchie, and G. A. C. Jones, Physica B **251**, 140 (1998).
[4] J. Cunningham, V. I. Talyanskii, J. M. Shilton, M. Pepper, M. Y. Simmons, and D. A. Ritchie, Phys. Rev. B **60**, 4850 (1999).
[5] J. Cunningham, V. I. Talyanskii, J. M. Shilton, M. Pepper, A. Kristensen, and P. E. Lindelof, Physica B **280**, 493 (2000).
[6] J. Cunningham, V. I. Talyanskii, J. M. Shilton, M. Pepper, A. Kristensen, and P. E. Lindelof, J. Low Temp. Phys. **118**, 555 (2000).
[7] J. Cunningham, V. I. Talyanskii, J. M. Shilton, M. Pepper, A. Kristensen, and P. E. Lindelof, Phys. Rev. B **62**, 1564 (2000).
[8] J. T. Janssen and A. Hartland, Physica B (to be published).
[9] J. Ebbecke, G. Bastian, M. Blöcker, K. Pierz, and F. J. Ahlers, cond-mat/0006487 (unpublished).
[10] H. Pothier, P. Lafarge, C. Urbina, D. Esteve, and M. H. Devoret, Europhys. Lett. **17**, 249 (1992).
[11] R. L. Kautz, M. W. Keller, and J. M. Martinis, Phys. Rev. B **60**, 8199 (1999).
[12] J. E. Cunningham, Ph.D. thesis, University of Cambridge, 2000.
[13] P. A. Maksym, Phys. Rev. B **61**, 4727 (2000).
[14] C. Zener, Proc. R. Soc. London, Ser. A **137**, 696 (1932); L. Landau, Phys. Z. Sowjetunion **2**, 46 (1932).
[15] K. Flensberg, Q. Niu, and M. Pustilnik, Phys. Rev. B **60**, 16 291 (1999).
[16] G. R. Aizin, G. Gumbs, and M. Pepper, Phys. Rev. B **58**, 10 589 (1998).
[17] G. Gumbs, G. R. Aizin, and M. Pepper, Phys. Rev. B **60**, 13 954 (1999).
[18] J. H. Davies and I. A. Larkin, J. Appl. Phys. **77**, 4504 (1995).
[19] J. M. Shilton, Ph.D. thesis, University of Cambridge, 1997.
[20] E. Wigner, Phys. Rev. **46**, 1002 (1934).
[21] R. S. Crandall and R. Williams, Phys. Lett. **34A**, 404 (1971).
[22] S. Kirkpatrick, C. D. Gelatt, and M. P. Vecchi, Science **220**, 671 (1983); S. Kirkpatrick, J. Stat. Phys. **34**, 975 (1984).
[23] V. M. Bedanov and F. M. Peeters, Phys. Rev. B **49**, 2667 (1993).
[24] F. Bolton and U. Rössler, Superlattices Microstruct. **13**, 139 (1993).
[25] A. S. Dzurak, C. J. B. Ford, M. Pepper, J. E. F. Frost, D. A. Ritchie, G. A. C. Jones, H. Ahmed, and D. G. Hasko, Phys. Rev. B **45**, 6309 (1992).
[26] See for reference D. V. Averin and K. K. Likharev, in *Mesoscopic Phenomena in Solids*, edited by B. Altshuler, P. A. Lee, and R. Webb (Elsevier, Amsterdam, 1991).
[27] S. T. Chui and K. Esfarjani, Phys. Rev. B **44**, 11 498 (1991).
[28] N. J. Appleyard, J. T. Nicholls, M. Y. Simmons, W. R. Tribe, and

M. Pepper, Phys. Rev. Lett. **81**, 3491 (1998).
[29] P. J. Price, J. Appl. Phys. **53**, 6863 (1982).
[30] M. Imada, J. Phys. Soc. Jpn. **53**, 3770 (1984).
[31] B. Tanatar and D. M. Ceperley, Phys. Rev. B **39**, 5005 (1988).
[32] L. D. Hallam, N. A. Bruce, and P. A. Maksym, Surf. Sci. **361/362**, 648 (1996).
[33] P. A. Maksym, Europhys. Lett. **31**, 405 (1995).
[34] F. Bolton, Phys. Rev. B **54**, 4780 (1996).
[35] F. Bolton, Dissertation zur Erlangung des Doktorgrades der Naturwissenschaften (Dr. rer. nat.) der naturwissenschaften Fakultät II—Physik der Universität Regensburg, 1994.
[36] M. Büttiker, Phys. Rev. B **41**, 7905 (1990).
[37] S. Habib, K. Shizume, and W. H. Zurek, Phys. Rev. Lett. **80**, 4361 (1998).
[38] John Preskill, *Lecture Notes on Quantum Information and Computation*, available at http://www.theory.caltech.edu/preskill/ph229